Chapter-IV

Analytical solution for Transient MHD flow through a Darcian porous regime in a Rotating System

Some part of this chapter has been published in the UGC approved journal entitled- International Journal of Engineering Research and Application, Volume 7- Issue 4 (Part-IV), April 2017, PP 85-89

4.1 Introduction:

The study of flow problems, which involve the interaction of several phenomena, has a wide range of applications in the field of science and technology. One such study is related to the effects of MHD free convection flow, which plays an important role in agriculture, engineering and petroleum industries. The problem of free convection under the influence of magnetic field has attracted the interest of many researchers because of its significant applications in geophysics and astrophysics. In view of these applications, Eckert and Drake (1972) have done pioneering work on heat and mass transfer. Elbashbeshy (1997) studied heat and mass transfer along a vertical plate under the combined buoyancy effects of thermal and species diffusion, in the presence of the magnetic field. Helmy (1998) presented the effects of magnetic field for an unsteady free convective flow past a vertical porous plate. Soundalgekar (1982) analyzed the problem of free convection effects on flow past a uniformly accelerated vertical plate under the action of transversely applied magnetic field with mass transfer. Kim (2000) investigated unsteady MHD convective heat transfer past a semi-infinite vertical porous moving plate with variable suction by assuming that the free stream velocity follows the exponentially increasing small perturbation law. The analytical solution of heat and mass transfer on the free convective flow of a viscous incompressible fluid past an infinite vertical porous plate in presence of transverse sinusoidal suction velocity and a constant free stream velocity was presented by Ahmed (2009). Also, Ahmed and Liu (2010) analyzed the effects of mixed convection and mass transfer of three-dimensional oscillatory flow of a viscous incompressible fluid past an infinite vertical porous plate in presence of transverse sinusoidal suction velocity oscillating with time and a constant free stream velocity by use of classical perturbation technique.

Convective heat/mass transfer flow in a saturated porous medium has gained growing interest. This fact has been motivated by its importance in many engineering applications such as building thermal insulation, geothermal systems, food processing and grain storage, solar power collectors, contaminant transport in groundwater, casting in manufacturing processes, drying processes, nuclear waste, just to name a few. A theoretical and experimental work on this subject can be found in the recent monographs by Ingham and Pop (1998) and Nield and Bejan (1998). Suction/blowing on convective heat transfer over a vertical permeable surface embedded in a porous medium was analyzed by Cheng (1977). In that work an application to warm water discharge along the well or fissure to an aquifer of infinite extent is discussed. Kim and Vafai (1989) analyzed the buoyancy driven flow about a vertical plate for constant wall temperature and heat flux. Raptis and Singh (1985) studied flow past an impulsively started vertical plate in a porous medium by a finite difference method. Ahmed (2010) studied the effect of transverse periodic permeability oscillating with time on the free convective heat transfer flow of a viscous incompressible fluid through a highly porous medium bounded by an infinite vertical porous plate subjected to a periodic suction velocity.

Rotating flow of electrically conducting viscous incompressible fluids has gained considerable attention because of its numerous applications in physics and engineering which are directly governed by the action of Coriolis and magnetic forces. In geophysics it is applied to measure and study the positions and velocities with respect to a fixed frame of reference on the surface of earth which rotate with respect to an inertial frame in the presence of its magnetic field. Injection/suction effects have also been studied extensively for horizontal porous plate in rotating frame of references by Ganapathy (1994), Mazumder (1991), Mazumder *et al.* (1976). Singh and Sharma (2001) studied the effect of the permeability of the porous medium on the three dimensional Couette flow and heat transfer. Moreover, Ahmed and Joaquin (2011) investigated the effects of Hall current, magnetic field, rotation of the channel and suction-injection on the oscillatory free convective MHD flow in a rotating vertical porous channel when the entire system rotates about an axis normal to the channel plates and a strong magnetic field of uniform strength is applied along the axis of rotation.

In the present problem an attempt has been made to study the effects of the permeability of the porous medium and rotation of the system on the free convective heat and mass transfer flow through a highly porous medium when the temperature of the surface varies with time about a non-zero constant mean and the temperature at the free stream is constant. The entire system rotates about an axis perpendicular to the planes of the plates. Such flows are very important in geophysical and astrophysical problems.

4.2 Mathematical Formulation:

The unsteady flow model of a viscous incompressible fluid through a porous medium occupying a semi-infinite region of the space bounded by a vertical infinite porous surface in a rotating system under the action of a uniform magnetic field applied normal to the direction of flow has been analyzed. The temperature of the surface varies with time about a non-zero constant mean and the temperature at the free stream is constant. The porous medium is, in fact, a non-homogenous medium which may be replaced by a homogenous fluid having dynamical properties equal to those of a non-homogenous continuum. Also, we assume that the fluid properties are not affected by the temperature and concentration differences except by the density ρ in the body force term; the influence of the density variations in the momentum and energy equations is negligible.

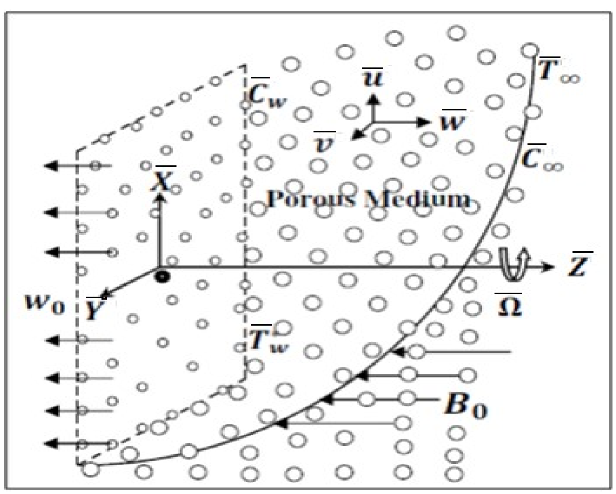

Fig. 4.2 (i): Sketch of the physical problem

The vertical infinite porous plate rotates in unison with a viscous fluid occupying the porous region with the constant angular velocity $\bar{\Omega}$ about an axis which is perpendicular to the vertical plane surface. The Cartesian coordinate system is chosen such that $\bar{X}$, $\bar{Y}$ axes respectively are in the vertical upward and perpendicular directions on the plane of the vertical porous surface $\bar{z} = 0$ while $\bar{Z}$-axis is normal to it as shown in Fig. 4.2(i). With the above frame of reference and assumptions, the physical variables, except the pressure $\bar{p}$ are functions of $\bar{z}$ and time $\bar{t}$ only. Consequently, the equations expressing the conservation of mass, momentum and energy and the equation of mass transfer, neglecting the heat due to viscous dissipation which is valid for small velocities and neglecting the pressure $\bar{p}$, are given by

$$\frac{\partial \overline{W}}{\partial \bar{z}} = 0 \tag{4.2.1}$$

$$\frac{\partial \bar{u}}{\partial \bar{t}} + \overline{W}\frac{\partial \bar{u}}{\partial \bar{z}} - 2\bar{\Omega}\bar{v} = g\beta(\bar{T} - \bar{T}_\infty) + g\bar{\beta}(\bar{C} - \bar{C}_\infty) + \nu\frac{\partial^2 \bar{u}}{\partial \bar{z}^2} - \frac{\nu}{\bar{K}}\bar{u} - \frac{\sigma B_0^2 \bar{u}}{\rho} \tag{4.2.2}$$

$$\frac{\partial \bar{v}}{\partial \bar{t}} + \overline{W}\frac{\partial \bar{v}}{\partial \bar{z}} + 2\bar{\Omega}\bar{u} = \nu\frac{\partial^2 \bar{v}}{\partial \bar{z}^2} - \frac{\nu}{\bar{K}}\bar{v} - \frac{\sigma B_0^2 \bar{v}}{\rho} \tag{4.2.3}$$

$$\frac{\partial \bar{T}}{\partial \bar{t}} + \overline{W}\frac{\partial \bar{T}}{\partial \bar{z}} = \frac{\kappa}{\rho C_p}\frac{\partial^2 \bar{T}}{\partial \bar{z}^2} \tag{4.2.4}$$

$$\frac{\partial \bar{C}}{\partial \bar{t}} + \overline{W}\frac{\partial \bar{C}}{\partial \bar{z}} = D\frac{\partial^2 \bar{C}}{\partial \bar{z}^2} \tag{4.2.5}$$

with the boundary conditions

$$\left\{\begin{array}{l} \bar{u} = 0, \quad \bar{v} = 0, \quad \bar{T} = \bar{T}_W + \varepsilon(\bar{T}_W - \bar{T}\infty)e^{i\omega t}, \quad \bar{C} = \bar{C}_W \quad at \quad \bar{z} = 0 \\ \\ \bar{u}, \bar{v} \to 0, \quad \bar{T} \to \bar{T}_\infty, \quad \bar{C} \to \bar{C}_\infty \quad as \quad \bar{z} \to \infty \end{array}\right\}, \tag{4.2.6}$$

where all the symbols have been defined in the Nomenclature section.

In a physically realistic situation, we cannot ensure perfect insulation in any experimental setup. There will always be some fluctuations in the temperature. The plate temperature is assumed to vary harmonically with time. It varies from $\overline{T}_W \pm \varepsilon(\overline{T}_W - \overline{T}_\infty)$ as t varies from 0 to 2π/ω. Since ε is small, the plate temperature varies only slightly from the mean value $\overline{T}_W$.

For constant suction, we have from Eq. (4.2.1) in view of (4.2.6)

$$\overline{W} = -W_0 \tag{4.2.7}$$

Considering $\overline{u} + i\overline{v} = \overline{U}$ and taking into account eq. (4.2.7), then Eqs. (4.2.2) and (4.2.3) can be written as

$$\frac{\partial \overline{U}}{\partial \overline{t}} - W_0 \frac{\partial \overline{U}}{\partial \overline{z}} + 2i\overline{\Omega}\overline{U} = g\beta v(\overline{T} - \overline{T}_\infty) + g\overline{\beta}(\overline{C} - \overline{C}_\infty)\frac{\partial^2 \overline{U}}{\partial \overline{z}^2} - \frac{v}{\overline{K}}\overline{U} - \frac{\sigma B_0^2 \overline{U}}{\rho} \tag{4.2.8}$$

Let us introduce the following non-dimensional quantities:

$$\left\{\begin{array}{l} z = \dfrac{W_0 \overline{z}}{v}, \quad U = \dfrac{\overline{U}}{W_0}, \quad t = \dfrac{\overline{t}\, W_0^2}{v}, \quad \omega = \dfrac{v\overline{\omega}}{\omega_0^2}, \quad \theta = \dfrac{\overline{T} - \overline{T}_\infty}{\overline{T}_W - \overline{T}_\infty}, \\ Pr = \dfrac{\rho v C_p}{\kappa}, \quad K = \dfrac{W_0^2 \overline{K}}{v^2}, \; Gr = \dfrac{vg\beta(\overline{T}_W - \overline{T}_\infty)}{W_0^3}, \quad \phi = \dfrac{\overline{C} - \overline{C}_\infty}{\overline{C}_W - \overline{C}_\infty}, \\ Gm = \dfrac{vg\overline{\beta}(\overline{C}_W - \overline{C}_\infty)}{W_0^3}, \quad \Omega = \dfrac{\overline{\Omega} v}{W_0^2}, \; M^2 = \dfrac{\sigma B_0^2 v}{\rho W_0^2}, \; Sc = \dfrac{v}{D}, \end{array}\right\}$$

In view of the above non-dimensional quantities, equations (4.2.8), (4.2.4) and (4.2.5) reduce, respectively to

$$\frac{\partial U}{\partial t} - \frac{\partial U}{\partial z} + i(2\Omega U) = Gr\theta + Gm\phi + \frac{\partial^2 U}{\partial z^2} - \left(K^{-1} + M^2\right)U \tag{4.2.9}$$

$$\frac{\partial \theta}{\partial t} - \frac{\partial \theta}{\partial z} = \frac{1}{Pr}\frac{\partial^2 \theta}{\partial z^2} \tag{4.2.10}$$

$$\frac{\partial \phi}{\partial t} - \frac{\partial \phi}{\partial z} = \frac{1}{Sc}\frac{\partial^2 \phi}{\partial z^2} \tag{4.2.11}$$

And the boundary conditions (4.2.6) become

$$\left\{\begin{array}{l} U=0, \quad \theta=1+\varepsilon e^{i\omega t}, \quad \phi=1 \quad at \quad z=0 \\ \\ U\to 0, \quad \theta\to 0, \quad \phi\to 0 \quad as \quad z\to\infty \end{array}\right\} \tag{4.2.12}$$

4.3 Method of Solution:

In order to reduce the system of partial differential equations (4.2.9)–(4.2.11) under their boundary conditions (4.2.12), to a system of ordinary differential equations in the non-dimensional form, we assume the following for velocity, temperature and concentration of the flow field as the amplitude ε (<< 1) of the permeability variations is very small:

$$\left\{\begin{array}{l} U(z,t)=U_0(z)+\varepsilon e^{i\omega t}U_1(z) \\ \\ \theta(z,t)=\theta_0(z)+\varepsilon e^{i\omega t}\theta_1(z) \\ \\ \phi(z,t)=\phi_0(z)+\varepsilon e^{i\omega t}\phi_1(z) \end{array}\right\} \tag{4.3.1}$$

Substituting (4.3.1) into the system (4.2.9)–(4.2.11) and equating harmonic and non-harmonic terms we get:

$$U_0''+U_0'-2i\Omega U_0-\left(K^{-1}+M^2\right)U_0=-(Gr\theta_0+Gm\phi_0) \tag{4.3.2}$$

$$U_1''+U_1'-\left[K^{-1}+M^2+i(\omega+2\Omega)\right]U_1=-(Gr\theta_1+Gm\phi_1) \tag{4.3.3}$$

$$\theta_0''+Pr\theta_0'=0 \tag{4.3.4}$$

$$\theta_1''+Pr\theta_1'-i\omega Pr\theta_1=0 \tag{4.3.5}$$

$$\phi_0''+Sc\phi_0'=0 \tag{4.3.6}$$

$$\phi_1''+Sc\phi_1'-i\omega Sc\phi_1=0 \tag{4.3.7}$$

The appropriate boundary conditions reduce to

$$\left\{\begin{array}{l} U_0(0)=0, \quad \theta_0(0)=1, \quad \phi_0(0)=1 \\ \\ U_1(0)=0, \quad \theta_1(0)=1, \quad \phi_1(0)=0 \\ \\ U_0(\infty)\to 0, \quad \theta_0(\infty)\to 0, \quad \phi_0(\infty)\to 0 \\ \\ U_1(\infty)\to 0, \quad \theta_1(\infty)\to 0, \quad \phi_1(\infty)\to 0 \end{array}\right\} \tag{4.3.8}$$

The solutions of the equations (4.3.2) to (4.3.7) subject to the boundary conditions (4.3.8) are:

$$U(z,t)=A_1e^{-Prz}+A_2e^{-Scz}+A_3e^{\psi_3 z}+\varepsilon\, e^{i\omega t}\, Gr\frac{(e^{\psi_5 z}-e^{\psi_1 z})}{(\psi_1-\psi_4)(\psi_1-\psi_5)} \tag{4.3.9}$$

$$\theta(z,t)=e^{-Prz}+\varepsilon\, e^{i\omega t}e^{\psi_1 z} \tag{4.3.10}$$

$$\phi(z,t)=e^{-Scz} \tag{4.3.11}$$

Now, it is convenient to write the primary and secondary velocity fields, in terms of the fluctuating parts, separating the real and imaginary part from equations (4.3.9) and (4.3.10) and taking only the real parts as they have physical significance, the velocity and temperature distribution of the flow field can be expressed in fluctuating parts as given below.

$$\frac{u}{w_0}=u_0+\varepsilon(\,N_r cos\,\omega t-N_i sin\,\omega t\,) \tag{4.3.12}$$

$$\frac{v}{w_0}=v_0+\varepsilon(\,N_r sin\,\omega t+N_i cos\,\omega t\,) \tag{4.3.13}$$

Where $u_0+iv_0=U_0$ and $N_r+iN_i=U_1$.

Hence, the expressions for the transient velocity profiles for $\omega t=\frac{\pi}{2}$ are given by

$$\frac{u}{w_0}\left(z,\frac{\pi}{2\omega}\right)=u_0(z)-\varepsilon N_i(z) \text{ and}$$

$$\frac{v}{w_0}\left(z,\frac{\pi}{2\omega}\right)=v_0(z)-\varepsilon N_r(z).$$

Skin Friction

The skin friction at the plate z = 0 is given by

$$\tau=\left.\frac{dU}{dZ}\right|_{z=0}=\left.\frac{dU_0}{dZ}\right|_{z=0}+\varepsilon\, e^{i\omega t}\left.\frac{dU_1}{dZ}\right|_{z=0}$$

$$=(-PrA_1-A_2Sc+A_3\psi_3)-\varepsilon e^{i\omega t}\frac{Gr}{(\psi_1-\psi_4)} \tag{4.3.14}$$

Rate of Heat Transfer

The heat transfer coefficient in terms of the Nusselt number at the plate z = 0 is given by

$$Nu=\left.\frac{d\theta}{dZ}\right|_{z=0}=\left.\frac{d\theta_0}{dZ}\right|_{z=0}+\varepsilon\, e^{i\omega t}\left.\frac{d\theta_1}{dZ}\right|_{z=0}=-Pr++\varepsilon\, e^{i\omega t}\psi_1 \tag{4.3.15}$$

The constants A_1 to A_3, ψ_1 to ψ_5 , N_i, N_r have been presented in the Appendix section.

4.4 Results and Discussion:

The problem of unsteady MHD free convective flow with heat and mass transfer effects in a rotating porous medium has been considered. The solutions for primary and secondary velocity field, temperature field and concentration profiles are obtained using the perturbation technique. The effects of flow parameters such as the magnetic parameter *M*, porosity parameter *K* and the rotation parameter **Ω** on the transient velocity profiles u/w_0 and v/w_0 have been studied analytically and presented with the help of Figs. 4.4. (i) to 4.4.(iii) and 4.4. (iv) to 4.4. (v). The effects of flow parameters on concentration profiles have been presented with the help of Fig. 4.4.

(vi). Further, the effects of flow parameters on the rate of heat transfer have been discussed with the help of Table 4.4 (*a*).

Primary Velocity Profile (u/w_o)

From equations (4.3.9), (4.3.10) and (4.3.11), it is observed that the steady part of the velocity field has a three layer character. These layers may be identified as the thermal layer arising due to interaction of the thermal field and the velocity field and is controlled by the Prandtl number; the concentration layer arising due to the interaction of the concentration field and the velocity field, and the suction layer as modified by the rotation and the porosity of the medium. On the other hand, the oscillatory part of the velocity field exhibits a two layer character. These layers may be identified as the modified suction layers, arising as a result of the triangular interaction of the **Coriolis force** and the unsteady convective forces with the porosity of medium.

With a rise in M, from 0, 5, 10 through 15 to 20 there is a strong reduction in magnitude of the primary velocity across the boundary layer. A velocity peak arises close to the wall for all profiles. The magnetic parameter is found to decelerate the primary velocity of the flow field to a significant amount due to the magnetic pull of the Lorentizian hydromagnetic drag force acting on the flow field. With constant M value (= 5.0), as the rotation parameter Ω is increased from 0.0 through 5.0, 10.0, 15.0 to 20.0, there is a distinct depression in velocity field i.e. the flow is decelerated. Conversely, an increase in porosity parameter K from 0.1, 0.3 through 0.5 to 1.0 the flow velocity is accelerated near the plate and then steadily reduces to zero in the free stream. Irrespective of M or Ω or K value, it is important to highlight that there is a flow reversal i.e. back flow has been seen in the boundary layer regime. The velocity u, sustains negative values throughout motion in boundary layer.

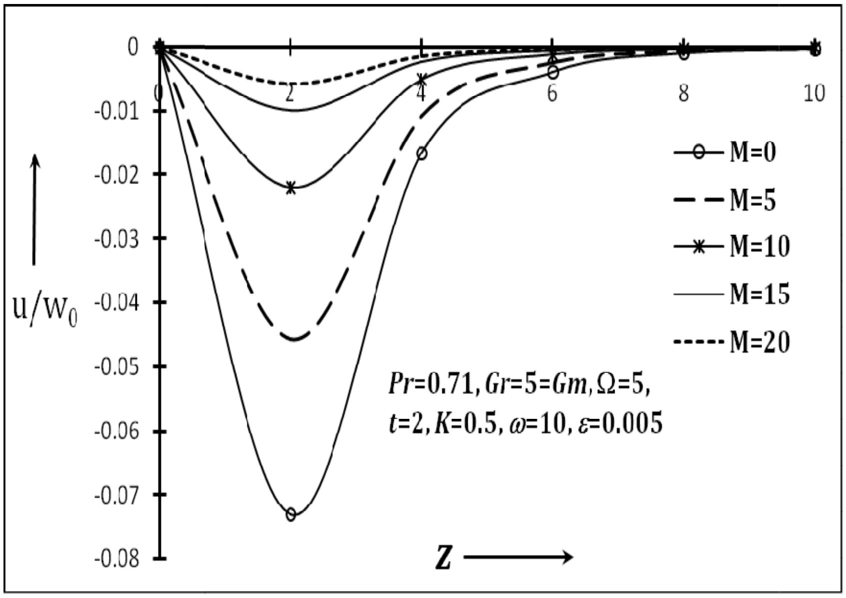

Fig. 4.4 (i): Effects of *M* on primary velocity profiles against *Z*

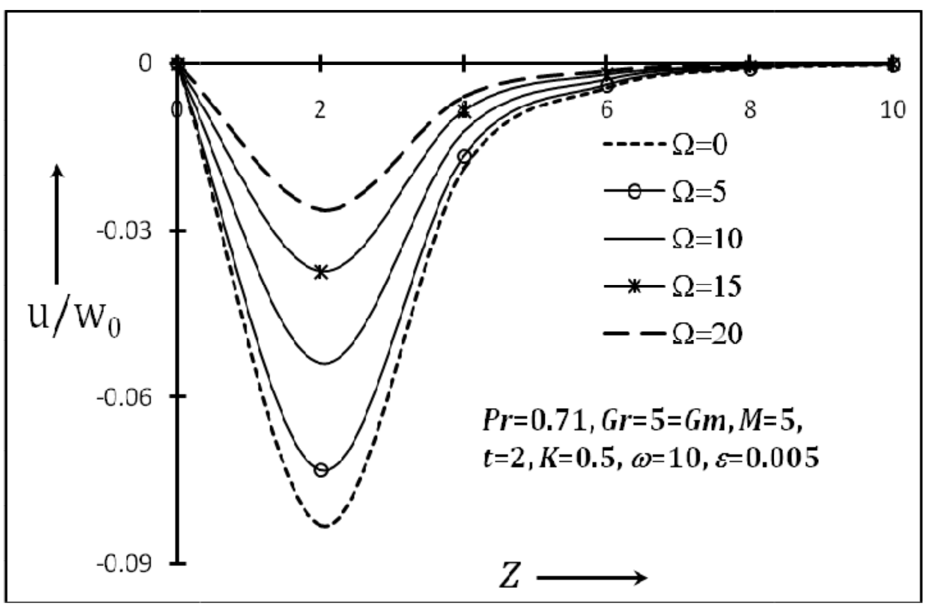

Fig. 4.4 (ii): Effects of Ω on primary velocity profiles against *Z*

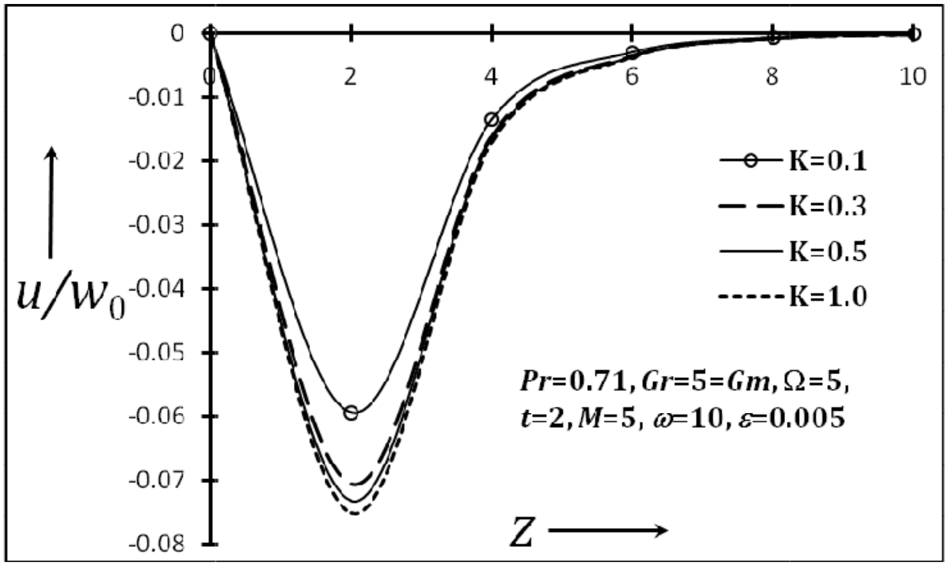

Fig. 4.4 (iii): Effects of *K* on primary velocity profiles against Z

Secondary Velocity Profile (v/w_o)

The Secondary velocity profiles are shown in Figs. 4.4 (iv) to 4.4 (v) for various values of the magnetic field (Hartmann number) and rotation parameter. This is indeed the trend observed in Fig. 4.4 (iv) where a strong deceleration in the flow is achieved with an increase in *M* from 0.0 (non-conducting case i.e. Lorentz force vanishes) through 1.0, 2.0, 3.0 to 5.0. It is observed from Fig. 4.4 (v) that the secondary velocity profiles increases when there is an increase in rotation parameter of the system. Significantly, the velocity profiles show the opposite trend to the primary velocity (Fig. 4.4 (ii)) when there is an increase in the rotation parameter. In no case however there is flow reversal i.e. velocities remain positive through the boundary layer.

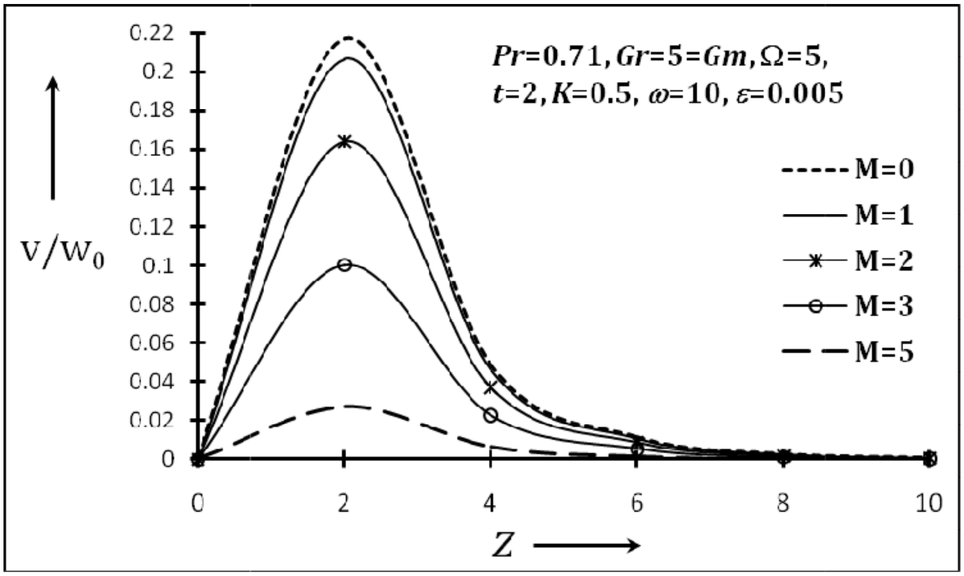

Fig. 4.4 (iv): Effects of *M* on secondary velocity profiles against *Z*

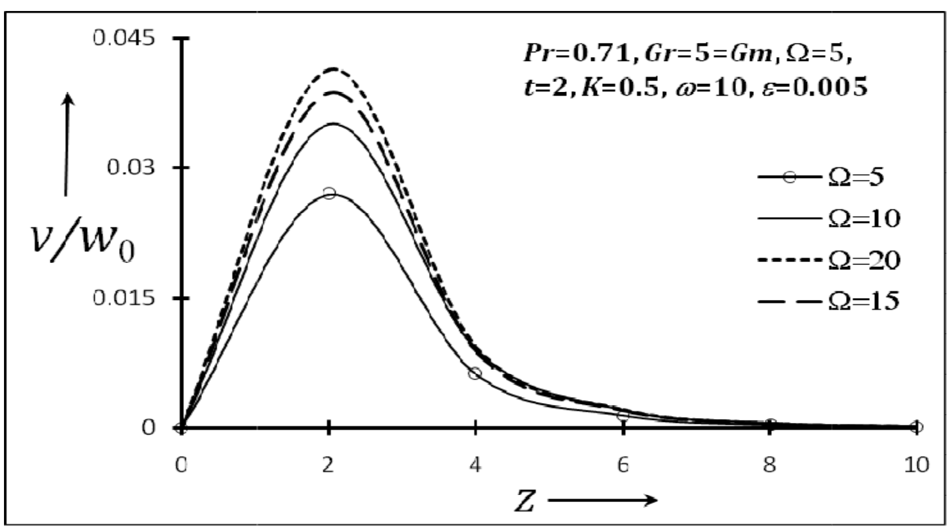

Fig. 4.4 (v): Effects of Ω on secondary velocity profiles against Z

Concentration Profiles (ϕ)

In Fig. 4.4 (vi), the concentration profiles ($\emptyset$) for various values of the Schmidt number are presented. The values of the Schmidt number *Sc* are chosen in such a way that they represent the diffusing chemical species of most common interest in air. For example, the values of Sc for H_2, H_20, NH_3, propyl benzene and helium in air are 0.22, 0.60, 0.78, 2.62 and 0.30, respectively as reported by Perry (1963). It is seen that the concentration profiles are decreased with an increase in the Schmidt number. It is noted that for heavier diffusing foreign species i.e. increasing the Schmidt number reduces the concentration in both magnitude and extent and thinning of concentration boundary layer occurs.

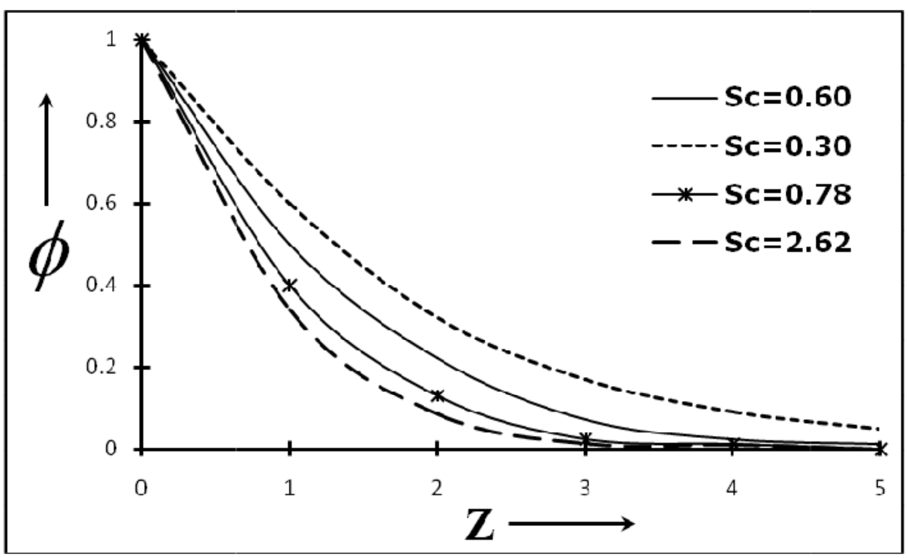

Fig. 4.4 (vi): Effects of Sc on concentration distribution

Skin Friction coefficient

The distribution of skin friction coefficients are explained in Figs. 4.4 (vii) to 4.4 (viii) for different values of the magnetic field, rotation parameter and porosity parameter. Inspection shows that increasing rotation (Ω) reduces skin friction. Increasing porosity (*K)* is found to increase the skin friction, consistency with earlier discussion for the velocity response (Fig. 4.4 (iii)). Flow reversal is observed i.e. skin friction becomes negative in both the figures 4.4 (vii) and 4.4 (viii). Clearly all profiles decay as *M* is increased since larger Hartmann number corresponds to greater magnetohydrodynamic drag which decelerates the flow.

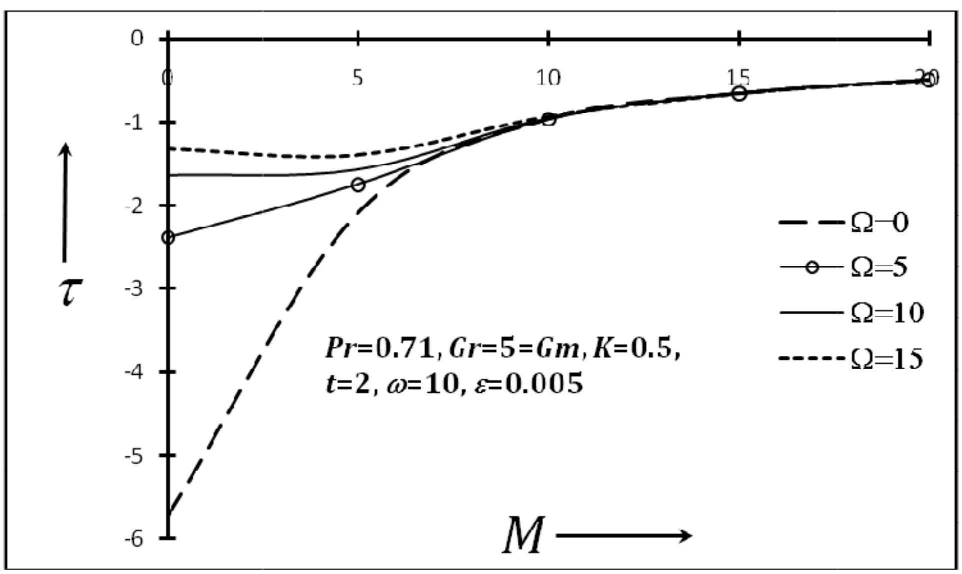

Fig. 4.4 (vii): Effects of Ω on skin friction against *M*

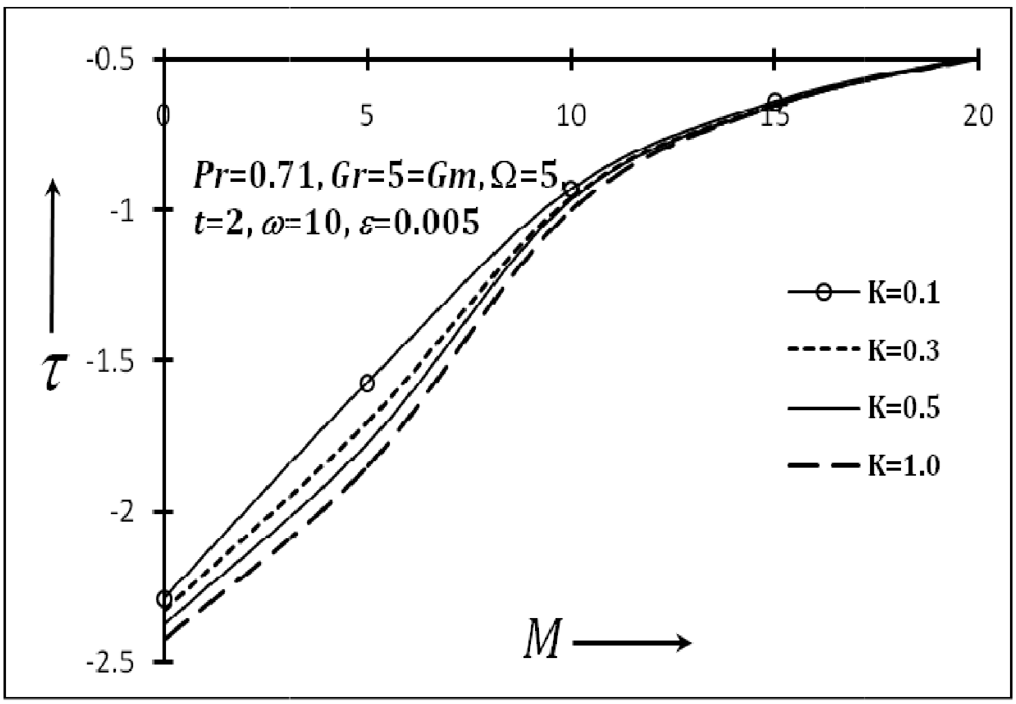

Figure 4.4 (viii): Effects of K on skin friction against *M*

Rate of Heat Transfer (*Nu*)

Table 4.4 (a): Heat transfer coefficient when $\varepsilon = 0.005$, in the case air and water:

			Pr = 0.71 (Air)	Pr = 7.0 (Water)
ω	T	M	Nu	Nu
2	2	2	0.34410	3.71514
2	2	3	0.37135	3.80426
3	2	3	0.80371	4.37293
3	3	3	0.03704	2.10853
3	3	4	0.02472	2.05830
4	3	4	0.90514	4.43715
4	4	4	0.07632	2.35304

Table 4.4 (*a*) shows the magnitude of the heat transfer coefficient for different values of ω, t and M. An increase either in the Hartmann number (M) or time (t) the magnitude of the heat transfer coefficient is reduced for both the cases of air and water. However, the heat transfer coefficient is escalated due to an increase in the frequency parameter (ω). Significantly, it is observed that the heat transfer coefficient in the case of water for any particular values of ω, t and M is much higher than that of air.

4.5 Conclusions:

The present theoretical analysis brings out the following results of physical interest on the primary and secondary velocities, concentration profiles, skin friction and rate of heat transfer of the flow field for a rotating system in a saturated porous regime:

- It is noticed that all the velocity profiles are increased steadily near the plate and thereafter they show a constant decrease and reach the value zero at the free stream.
- The magnetic as well as rotation parameter is found to decelerate the primary velocity of the flow field.
- The porosity drag force has an effect in accelerating both the primary velocity profiles and the skin friction as well.
- There is a clear back flow for all the primary velocity profiles.
- The secondary velocity profiles and skin friction coefficient are opposite to each other due to the effect of rotation.
- The magnetic parameter has the effect of decreasing both the heat transfer profiles and the skin friction as well.
- The presence of foreign species reduces the concentration boundary layer and further reduction occurs with increasing values of the Schmidt number.
- The Prandtl number and the frequency parameter have the effect of increasing the heat transfer coefficient.